Effects of substrate heating and biasing on nanostructural evolution of non-epitaxially grown TiN nano-films

T. Q. Li [a)], S. Noda [a)], F. Okada, and H. Komiyama

Department of Chemical System Engineering, University of Tokyo, 7-3-1 Hongo, Bunkyo-ku, Tokyo 113-8656, JAPAN

(Received

[a)]Author to whom correspondence should be addressed; electronic mail: litg@chemsys.t.u-tokyo.ac.jp; noda@chemsys.t.u-tokyo.ac.jp

Abstract

The effects of substrate heating and substrate biasing on the initial stage of non-epitaxial heterogeneous growth of TiN on Si(111) was studied by using high-resolution transmission electron microscopy. Although TiN films deposited at room temperature (*RT*) undergo a transition from continuous, amorphous films to polycrystalline films with three-dimensional grains when the film thickness is increased from ~ 1 to 2 nm, crystallization occurred at a substrate temperature, T_s = 570 K, even for film thicknesses less than 1 nm. Compared with growth at T_s = *RT*, at T_s = 570 K the initial, lateral grain size was only slightly larger, and the grains tended to be spherical and discontinuous at higher film thickness. At a substrate bias voltage, V_b = -70 V, the grains were laterally larger and planar. At a film thickness of 50 nm, the films deposited at V_b = -70 V showed the thermodynamically favored (200) preferred orientation, whereas the films deposited at T_s = 570 K showed (111) preferred orientation with a weak (200) peak.

PACS numbers:

1. 68.55.Ac.

2. 68.55.Jk.

3. 81.15.Cd.

I. INTRODUCTION

Due to size miniaturization and density increase of integrated circuits (ICs), the thickness of the barrier layers (TiN, TaN, etc.) for metal interconnections (Al, Cu, etc.) must be reduced to less than 10 nm in order to reduce the resistivity of metal/barrier structures.[1] To develop such ultra-thin diffusion barriers, a detailed understanding of their initial growth mechanism is needed.

The barrier layers are often deposited non-epitaxially on either Si or SiO_2 substrates and form through crystal nucleation, grain growth, and coalescence. Many investigations have been made on the texture evolution[2-4] and homogeneous growth of TiN.[5-7] Unfortunately, little effort has been directed at understanding initial formation mechanisms of these non-epitaxial heterostructures.[8,9] Previous results indicated that TiN deposited onto Si by reactive sputtering undergoes a thickness-dependent crystal nucleation at room temperature.[9] Further studies are needed, therefore, to determine the effect of deposition parameters on the nonepitaxial, initial growth. For thick film growth (e.g., at micrometer-ordered thickness), substrate heating or biasing are known to favor the formation of (200) preferred orientation because this is the lowest surface energy existing for the (200) plane of NaCl-type crystal TiN films.[10] However, at the initial growth stage when the films have a thickness on the order of nanometers, the effects are more complicated due to non-epitaxtial heterogeneous nucleation and coalescence. In this work, the influences of substrate temperature, T_s, and bias voltage, V_b, on the initial film nanostructure are investigated by using high-resolution transmission electron microscopy (HRTEM).

II. EXPRIMENTS

TiN thin films were deposited using dc reactive magnetron sputtering. The sputter chamber had a base pressure of 5×10^{-6} Pa. The target was a 2-inch-diameter, 99.99% pure Ti plate, and the substrates on which the films were grown were (111) Si wafers. Before being loaded into the loading chamber, the wafers were treated chemically in a mixture of concentrated sulfuric acid and H_2O_2, and then dipped into a 1% HF solution to remove the contaminants and the native SiO_2 layer on the surface. After each chemical treatment, the wafers were washed in deionized water. Before deposition, the target was pre-sputtered for 5 min under the same conditions as for the TiN deposition. The substrate was shuttered with a rotating shuttering system during pre-sputtering. Deposition was done by rotating the shutter to a position where a hole in the shutter was in line between the target and the substrate. During deposition, the total pressure, P, in the sputtering chamber was maintained at P = 0.93 Pa, and the N_2 partial pressure, P_{N2} = 0.047 Pa. The substrate-to-target distance was fixed at 50 mm, and the discharge power to the Ti target was 69 W dc (260 V, 0.265 A). TiN films were deposited under these conditions without substrate heating (in this paper we refer to this condition as $T_s = RT$, where RT represents room temperature and 290 K < RT < 308 K), or at T_s = 570 K. The substrate bias voltage, V_b, was either a self-bias voltage, V_b = - 23 V, induced from the plasma, or was set to V_b = - 70 V. The ion current density at the substrate, determined from the current density-voltage characteristic of the substrate (not shown here), was estimated to be 0.57 $mAcm^{-2}$ (corresponding to an ion flux of 3.5×10^{15} $cm^{-2}s^{-1}$).

The nanostructure of the films was investigated with transmission electron microscopy (TEM: JEOL, JEM2010F, Japan) operated at 200 kV. HRTEM observations of plan-view and cross-sectional (XHRTEM) specimens were made.

The deposition rate was determined by measuring the film thickness (about 50 nm)

with a stylus profilometer (KLA-Tencor P-10, U.S.A.). The thickness of initial films, h_c, was calculated from the deposition rate (R) and time (t) as $h_c = R \times t$. The deposition rates at V_b = - 23 V and -70 V were 0.19 and 0.17 nm/s, respectively. The slightly lower deposition rate at V_b = - 70 V was presumably due to resputtering on the film surface.

The x-ray diffraction (XRD) (Rigaku RINT2400, Japan) analysis was done by using Cu $K\alpha$ radiation.

Additional details of our experimental setup are given elsewhere.[8, 9]

III. RESULTS

A. Growth at 570 K

Figs. 1 and 2 **(modify the arrows ?!)** show plan-view and cross-sectional HRTEM images of films deposited at T_s = 570 K (V_b = -23 V). Figs. 1(a) and 2(a) show films deposited for t = 4 s (h_c = 0.8 nm). Samples deposited at *RT* were continuous and amorphous, as determined by HRTEM.[9] However, samples deposited at T_s = 570 K exhibited crystal nuclei in the sub-nanometer-film. The XHRTEM images show that the nuclei were nearly spherical and that their height was about 2 nm, more than twice that of h_c. This implies that deposits aggregated at T_s = 570 K.

For t = 8.5 s (h_c = 1.6 nm), Figs. 1(b) and 2(b) show that the nuclei (grains) grew three dimensionally, resulting in a rougher film surface compared with films deposited at T_s = *RT*. (see Fig. 2 in Ref. 9)

Figs. 1(c) and 2(c) show that for t = 25 s (h_c = 4.8 nm), the grains grew large to come in contact with each other, resulting into a polycrystalline film with distinct grain boundaries. The SAED patterns indicate that the (do not use so many terms such as “nuclei”, “grains”, and “crystallites”) grains had random orientation both in-plane and

out-of-plane directions.

For h_c = 16 nm, the XRD results shown in Fig. 3(b) indicate that the film had a nearly random orientation and that the (200) intensity was stronger than that of the film deposited at T_s = *RT* [shown in Fig. 3(a)]. The intensity of the (200) peak remained unchanged with increasing h_c, whereas the intensity of the (111) peak increased rapidly with increasing h_c, and the film exhibited a (111) preferred orientation at h_c = 40 nm.

For T_s = 570 K, the XHRTEM images show an amorphous interlayer 0.9 nm thick between the deposits and the substrate, whereas for films deposited at T_s = *RT*, the interlayer thickness was less than 0.5 nm thick (see Fig. 2 in Ref. 9). XHRTEM and XPS analysis showed that the interlayer formed at T_s = *RT* and P_{N2} = 0.47 Pa was mainly SiN_x.[9] The formation of the thicker amorphous interlayer at T_s = 570 K may be due to enhanced inter-diffusion and/or oxidation of the Si surface when heated in the sputter-chamber before deposition of TiN. Fig. 2 indicates that there should be little Ti in the interlayer, because the contrast of the interlayer was much brighter than that of the TiN layer, and closer to that of Si. If the interlayer contained high concentrations of Ti, the relatively heavy Ti atoms would efficiently scatter electrons, and therefore darken the contrast of the layer.

Fig. 4 shows a correlation of the changes of the average lateral grain size with film growth at T_s = *RT* and T_s = 570 K. Each reported lateral grain size is an average of the measured size of more than 100 randomly-sampled grains from plan-view HRTEM images taken from a single film sample. The error bars represent the standard deviation of the lateral grain size. For T_s = 570 K, from h_c = 0.8 to 1.6 nm the lateral grain size increased from 2.2 to 3.0 nm, and the lateral grain size was almost the same as the grain height. This indicates three-dimensional grain growth and is identical to the XHRTEM

results shown in Fig. 2. At h_c = 4.8 nm, the lateral grain growth rate decreased because the grains came into contact with each other, and mainly grew vertically.

Fig. 4 indicates that compared with the grains deposited at T_s = 570 K, the grains grown at T_s = *RT* were smaller and had lower lateral growth rate. This may be because of the lower adatom mobility and higher density of initial nucleation sites at the lower substrate temperature. The grains therefore came into contact with each other earlier in the film-growth process.

B. Growth under substrate biasing

Fig. 5 show results for TiN initial films deposited at V_b = -70 V (T_s = *RT*). Fig. 5(a) shows a plan-view HRTEM image together with SAED patterns for a film with h_c = 3.4 nm. The grains had an average lateral size of 5.9 nm, about twice the film thickness. As shown in Fig. 5(a), some grains with relatively large lateral size were (200) oriented. Fig. 5(b) shows an XHRTEM image for a film with h_c = 2.5 nm. The film was smooth and the grains were planar with a relatively large top surface area.

Fig. 6 shows the XRD spectra for h_c = 50 nm, and for V_b = -23 V (self-bias potential) and V_b = -70 V. For V_b = -23 and -70 V, the film orientation was (200) and (111), respectively.

IV. DISCUSSION

Previously reported HRTEM results showed that at T_s = *RT* (V_b = -23 V), the initial non-epitaxial growth of TiN on Si undergoes a thickness-dependent 3D crystal nucleation from an initial continuous, 2D amorphous layer.[9] For T_s = 570 K, crystallization occurred for h_c < 1 nm. This may be because with increasing T_s, the

adatom mobility increases, causing the formation of islands. With increasing T_s, the amount of film material required for the discontinuous islands to reach a critical height decreases, permitting crystal nucleation to occur in the initial stages of deposition.

The texture of the initial layers is affected by two important energy parameters: the film/substrate interfacial energy, $\gamma_i^{f/s}$, and the film surface energy, γ_s^f. The minimization of both $\gamma_i^{f/s}$ and γ_s^f is the primary driver for texture development in the initial stage. For epitaxial growth, lattice matching causes a large decrease in $\gamma_i^{f/s}$, and the deposited film orientation is determined by matching the orientation of the substrate. For non-epitaxial, heterogeneous growth, the initial film texture is mainly determined by minimization of γ_s^f. In the initial growth stage when the crystal nuclei (grains) are discontinuous, γ_s^f does not depend on the grain orientation and no orientation is preferred if the grains are non-wetting and spherical. This is consistent with previous results[9] and with the results shown in Section III that TiN growth at either $T_s = RT$ or 570 K shows no preferred orientation in the nucleation stage.

When the crystal grains grow large enough to contact each other, the continuous film tends to orient itself with the lowest surface-energy plane parallel to the substrate to minimize γ_s^f. At $T_s = RT$ and low ion irradiation, this thermodynamically favored transition does not occur to any significant degree, and the grains mainly grow vertically with an initial, random orientation. Because the (111) oriented grains have a higher growth rate than the other oriented grains, (111) oriented films are formed by the "evolutionary selection rule". [4, 8, 11]

When the films are deposited at T_s = 570 K, the grains tend to become spherical and discontinuous. In addition, the grains become continuous at a greater thickness than for $T_s = RT$. The evolutionary selection growth, which leads to (111) preferred orientation,

therefore occurs later than for T_s = *RT*. This delay in the occurrence of evolutionary selection growth might be the cause of the stronger intensity of the (200) orientation in the XRD spectra of films deposited at T_s = 570 K than for films deposited at T_s = *RT*.

Fig. 5 indicates that grains of the films deposited at V_b = -70 V have a larger lateral than vertical size, and are planar. For films deposited with substrate biasing the ions (such as Ar^+ and N_2^+, etc.) impinge on the film surface with higher kinetic energy. This higher ion energy at V_b = -70 V may cause the following effects on the film, resulting in the formation of planar grains. Higher ion energy:

(1) increases the mobility of the adatoms on the grain surface, thus promoting diffusion of atoms to the edges.

(2) promotes grain coalesce with adjacent grains, forming a planar shape.

(3) causes loosely bound ions on the surface of the grains to be resputtered, resulting in a denser film structure.

Due to their larger top than side area, to lower their surface energy planar grains may restructure into (200) orientation planes under energetic ion bombardment. The films show (200) preferred orientation at a thickness of 50 nm.

V. CONCLUSIONS

Although TiN films deposited at room temperature (T_s = *RT*) undergo a transition from continuous, amorphous layers to three-dimensional, crystalline layers, when the film thickness increased from ~ 1 to 2 nm, crystallization occurred at T_s = 570 K, even for film thicknesses less than 1 nm. Compared with growth at T_s = *RT*, at T_s = 570 K the initial grains tended to be spherical and discontinuous at higher film thickness. At a substrate bias voltage, V_b = -70 V, the grains were laterally larger and planar. The

different effects of T_s and V_b on TiN initial growth resulted in different textures at a film thickness of 50 nm

ACKNOWLEDGEMENTS

This work was supported, in part, by the New Energy and Industrial Technology Development Organization’s (NEDO) "Nanotechnology Program - Systemization of Nanotechnology Materials Program Results Project", of the Ministry of Economy, Trade, and Industry (METI), Japan, and by the Japan Society for the Promotion of Science (JSPS)’s "Grant-in-Aid for Creative Scientific Research - Establishment of Networked Knowledge System with Structured Knowledge for Future Scientific Frontier Project", of the Ministry of Education, Culture, Sports, Science and Technology (MEXT), Japan.

REFERENCES

[1]S. P. Murarka, R. J. Gutmann, A. E. Kaloyeros, and W. A. Lanford, Thin Solid Films **236**, 257 (1993).

[2]U. C. Oh and J. H. Je, J. Appl. Phys. **74**, 1692 (1993).

[3]J. Pelleg, L. Z. Zevin, and S. Lungo, Thin Solid Films **197**, 117 (1991).

[4]L. Hultman, J.-E. Sundgren, J. E. Greene, D. B. Bergstrom, and I. Petrov, J. Appl. Phys. **78**, 5395 (1995).

[5]F.H. Baumann, D.L. Chopp, T. Díaz de la Rubia, G.H. Gilmer, J.E. Greene, H. Huang, S. Kodambaka, P.O'Sullivan, and I. Petrov, MRS Bull. **26**, 182 (2001).

[6]S. Kodambaka, V. Petrova, A. Vailionis, P. Desjardins, D.G. Cahill, I. Petrov, J.E. Greene, Thin Solid Films **392**, 164 (2001).

[7]S. Kodambaka, V. Petrova, S.V. Khare, D. Gall, A. Rockett, I. Petrov, J.E. Greene, Phys. Rev. Lett. **89**, 176102-1 (2002).

[8]T. Q. Li, S. Noda, Y. Tsuji, T. Ohsawa, and H. Komiyama, J. Vac. Sci. Technol. A **20**, 583 (2002).

[9]T. Q. Li, S. Noda, and H. Komiyama, J. Vac. Sci. Technol. A, Sept/Oct, 2003 (in press).

[10]J. Pelleg, L. Z. Zevin, and S. Lungo, Thin Solid Films **197**, 117 (1991).

[11]J.E. Greene, J.-E. Sundgren, L. Hultman, I. Petrov and D.B. Bergstrom, Appl. Phys. Lett. **67**, 2928 (1996).

FIGURE CAPTIONS

Fig. 1 Plan-view TEM images and corresponding SAED patterns of TiN deposited at a temperature of 570 K for deposited film thicknesses of (a) 0.8 nm, (b) 1.6 nm, and (c) 4.8 nm.

Fig. 2 XHRTEM images of TiN deposited at a temperature of 570 K for deposited film thicknesses of (a) 0.8 nm, (b) 1.6 nm, and (c) 4.8 nm.

Fig. 3 XRD scans showing the effect of film thickness on preferred orientation of TiN deposited at (a) room temperature and (b) 570 K.

Fig. 4 Lateral grain size vs. film thickness.

Fig. 5 (a) Plan-view TEM image and corresponding SAED patterns of a 3.4-nm film and (b) XHRTEM image of a 2.5-nm film deposited at a bias voltage of V_b = -70 V.

Fig. 6 Effect of substrate bias voltage on the texture of 50-nm films.

Fig. 1

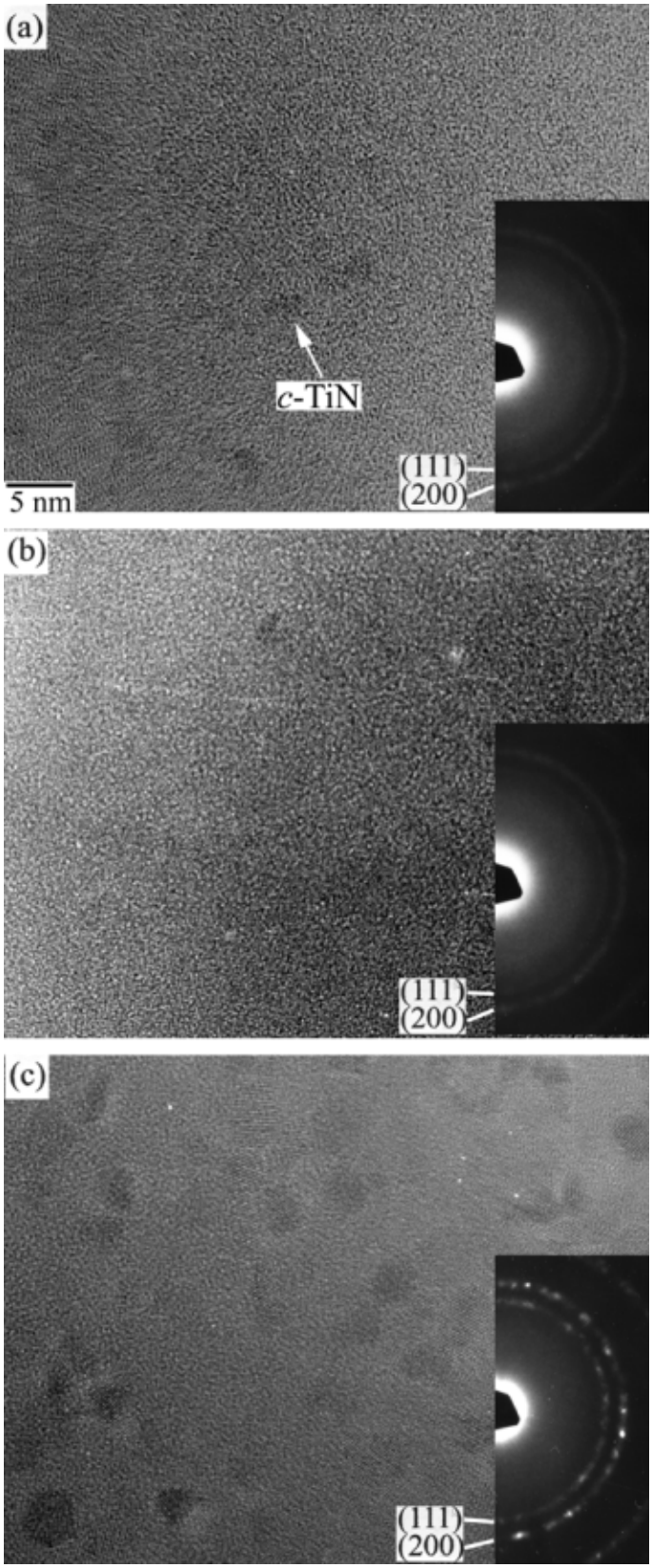

Fig. 2

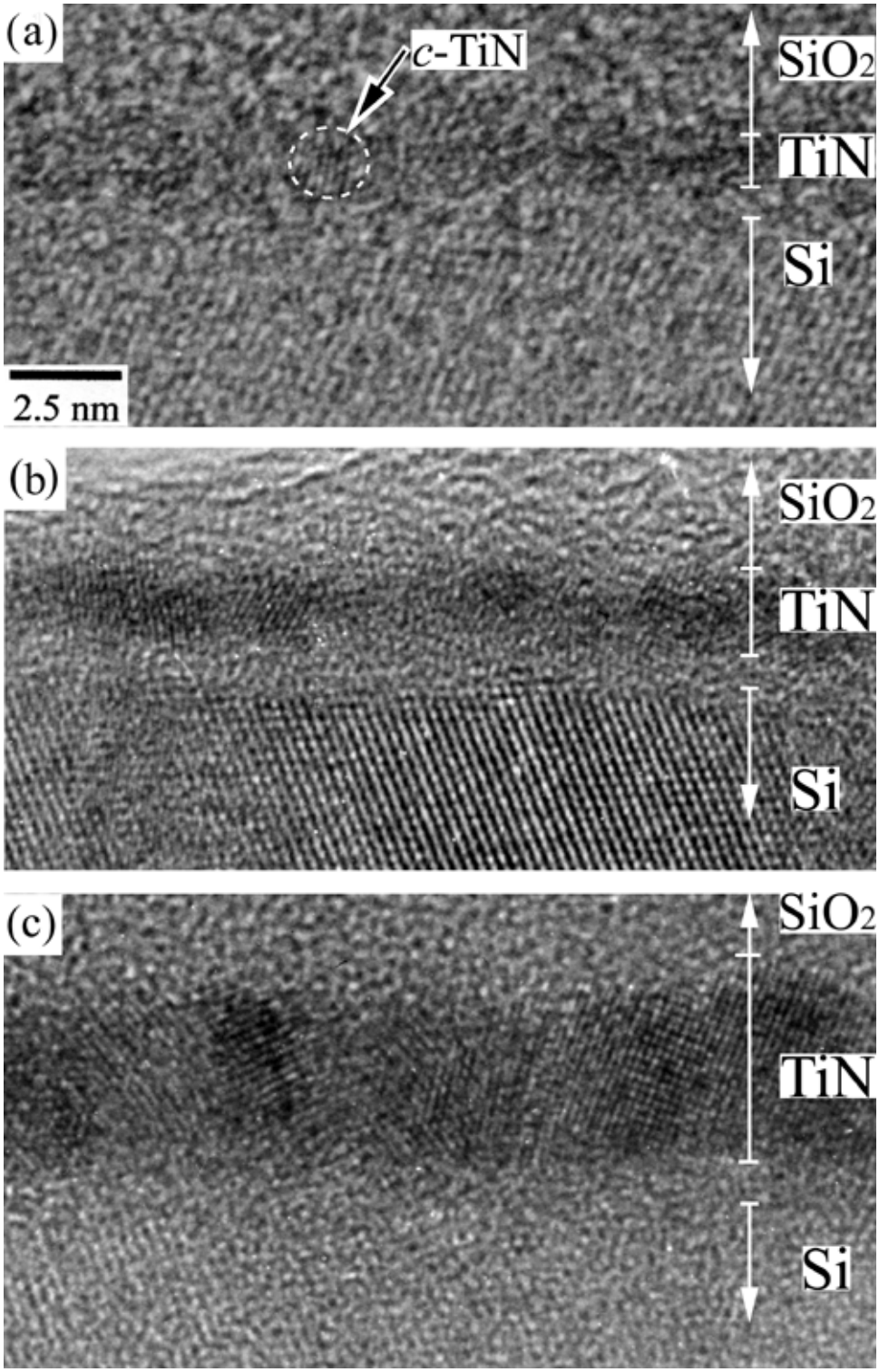

Fig. 3

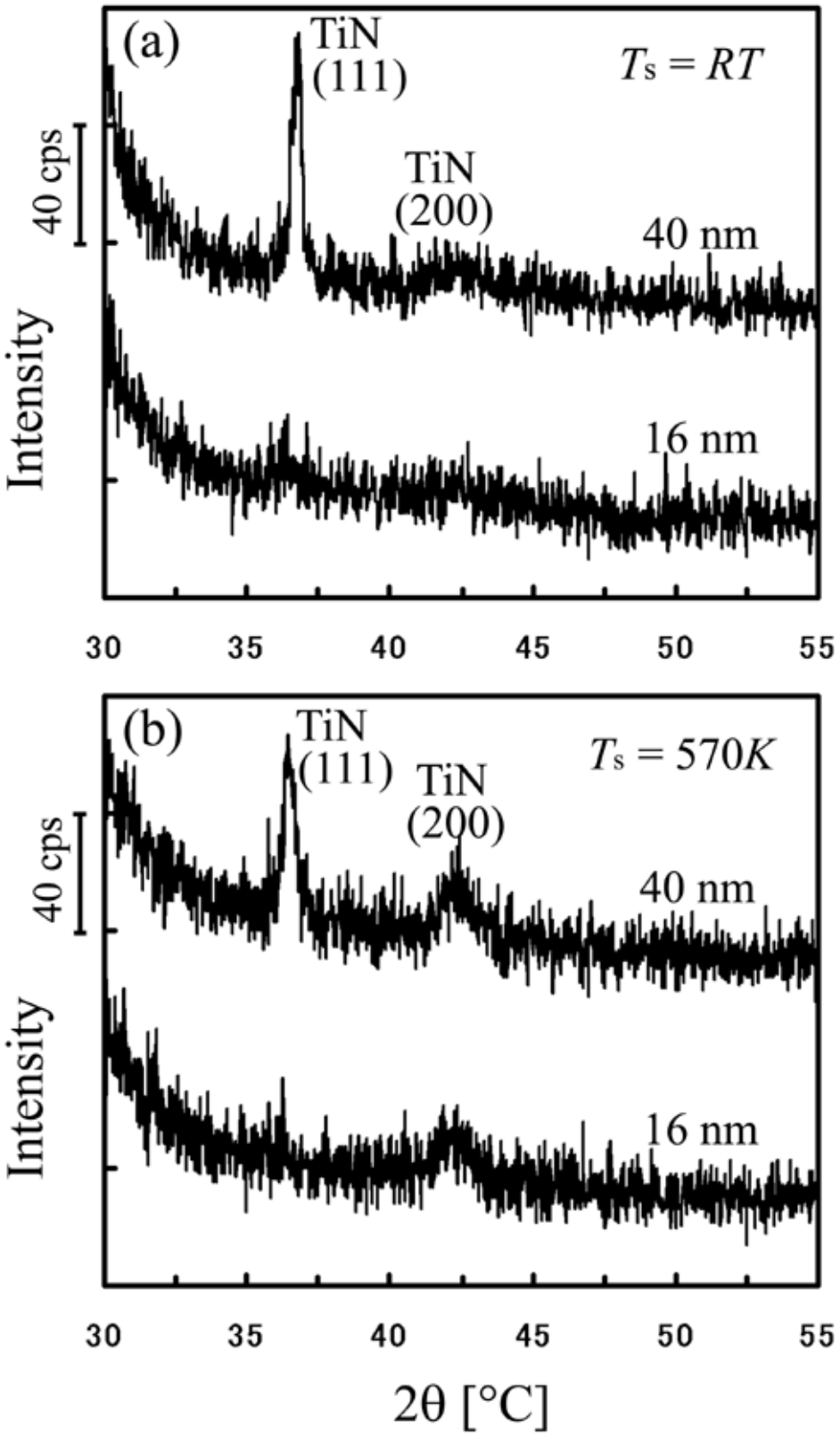
(a)
TiN
(111)
$T_s = RT$
TiN
(200)
40 nm
16 nm
40 cps
Intensity
30
35
40
45
50
55
(b)
TiN
(111)
TiN
(200)
$T_s = 570K$
40 nm
16 nm
40 cps
Intensity
30
35
40
45
50
55
2θ [°C]

Fig. 4

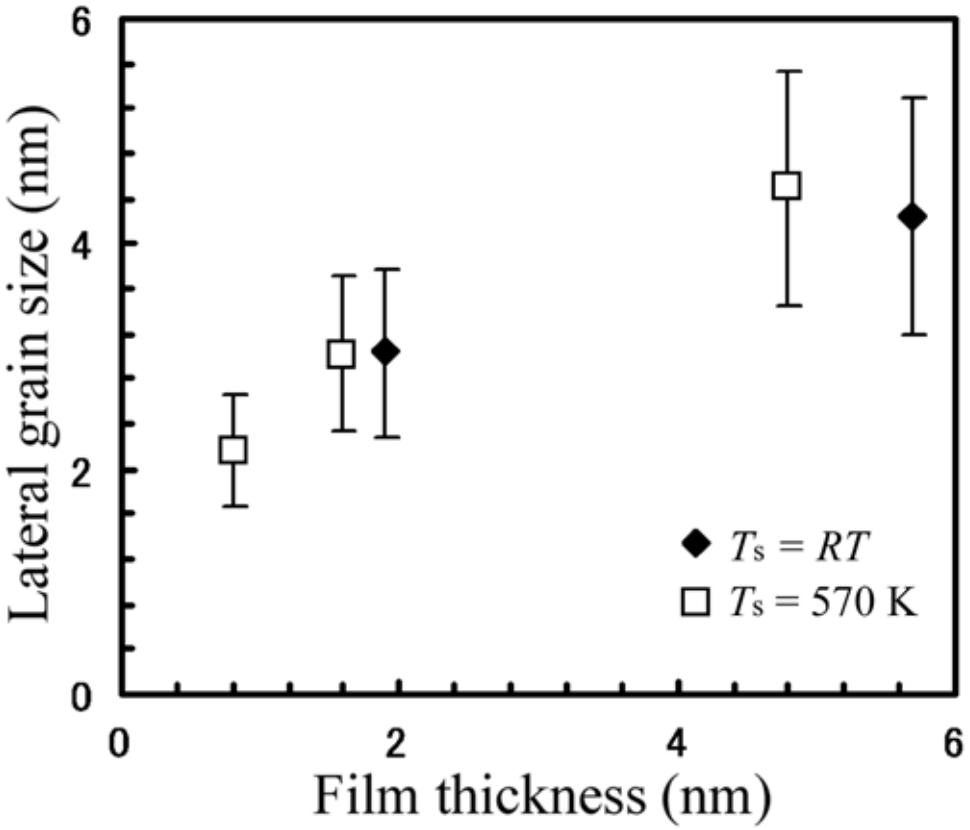

Fig. 5

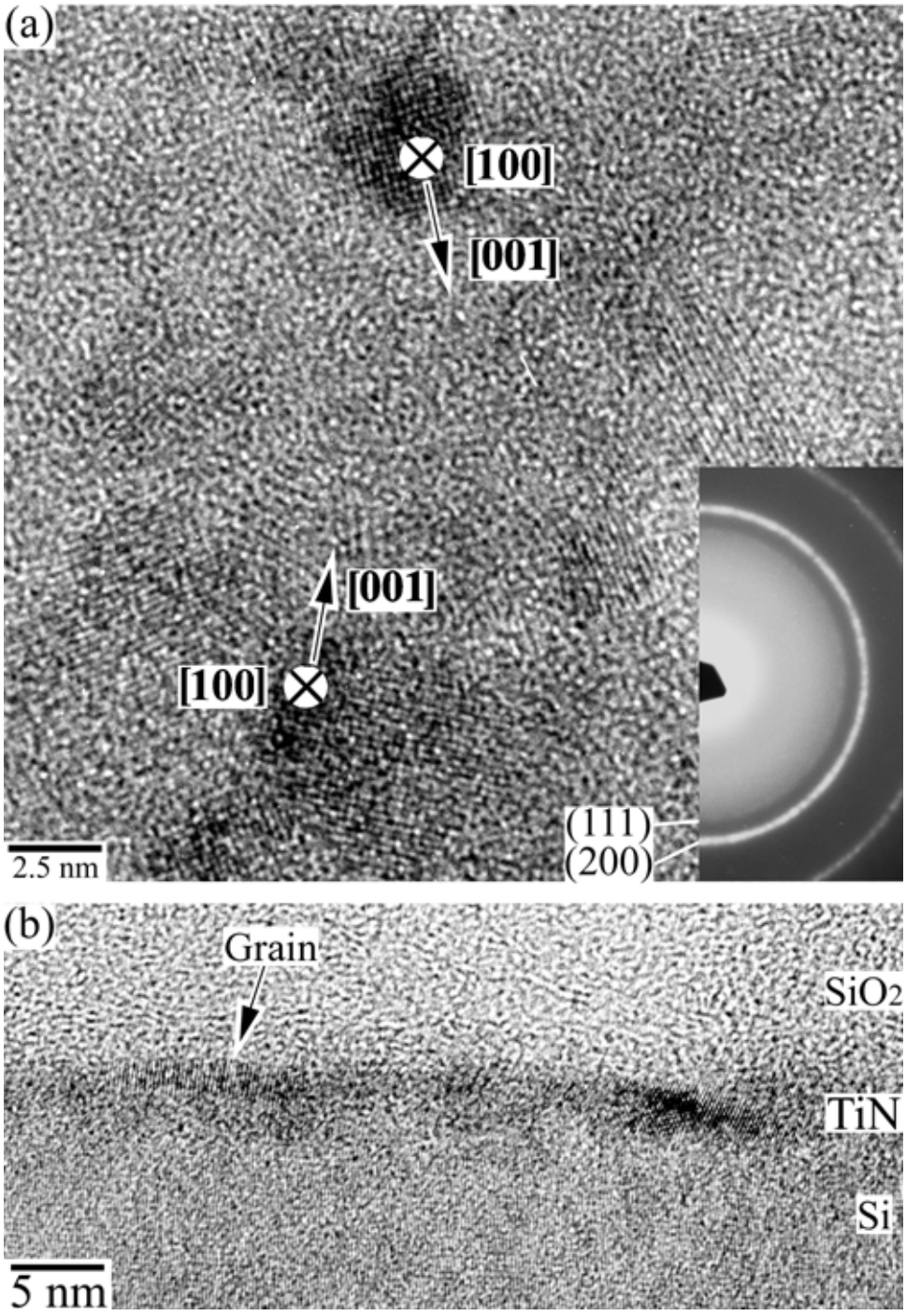

Fig. 6

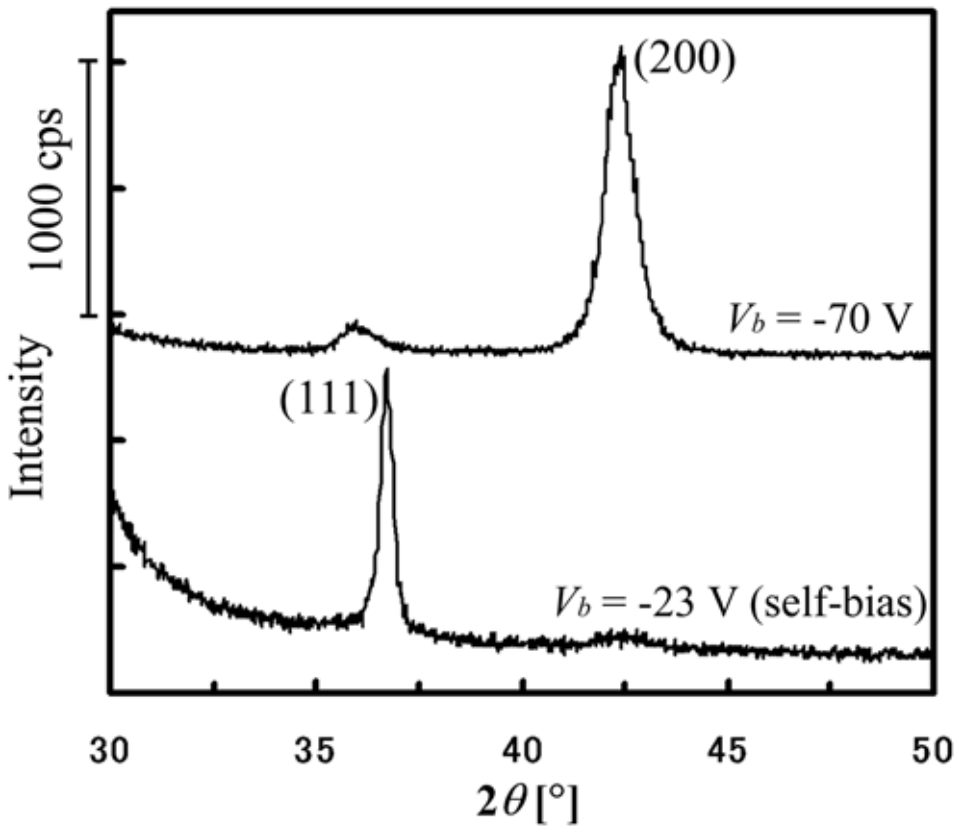
(200)
1000 cps
Intensity
V_b = -70 V
(111)
V_b = -23 V (self-bias)
30
35
40
45
50
2θ [°]